



ORIGINAL ARTICLE

Signaling pathway in development of *Camellia oleifera* nurse seedling grafting union

Jin-Ling Feng^{1,2} · Zhi-Jian Yang^{1,2} · Shi-Pin Chen¹ · Yousry A. El-Kassaby² · Hui Chen¹

Received: 25 November 2016 / Accepted: 31 May 2017 / Published online: 6 June 2017
© The Author(s) 2017. This article is an open access publication

Abstract

Key message The anatomical and physiological signaling pathways associated with successful scion-rootstock union in nurse seedling grafting of *Camellia oleifera* propagation are illustrated.

Abstract Grafting, the successful union between scion and rootstock, has practical and biological importance. Nurse seedling grafting, as those practiced for *Camellia oleifera*, often results in high cell division activity and affinity, and is usually associated with significant rootstock and scion anatomical structures changes. However, a comprehensive explanation of signaling pathways, and how they affect graft union development, is still largely unknown. The present study investigates the union formation process in *C.*

oleifera nurse seedling grafts and determines that it consists of six stages, namely, isolation layer formation, rootstock callus differentiation, scion callus differentiation, callus proliferation and connection, cambium differentiation and connection, and conducting tissue differentiation and connection, extending over a period of 35 days. Principal components analyses of the observed changes in physiology and protein expression identified three main factors contributing to the union formation process: cell proliferation, cell differentiation, and vascular bundle development. Further analysis showed that the regulation of the union formation process can be divided into two signaling pathways, namely, calcium and MAPK, which occur during vascular bundle development and cell proliferation and differentiation, respectively.

Communicated by Q. Han.

Electronic supplementary material The online version of this article (doi:[10.1007/s00468-017-1568-9](https://doi.org/10.1007/s00468-017-1568-9)) contains supplementary material, which is available to authorized users.

✉ Yousry A. El-Kassaby
y.el-kassaby@ubc.ca

✉ Hui Chen
zjchchenh@163.com

Jin-Ling Feng
fengjinling@fafu.edu.cn

Zhi-Jian Yang
yangzhijian@fafu.edu.cn

Shi-Pin Chen
fjcs@126.com

¹ College of Forestry, Fujian Agriculture and Forestry University, Fuzhou 350002, China

² Department of Forest and Conservation Sciences, Faculty of Forestry, University of British Columbia, Forest Sciences Centre, 2424 Main Mall, Vancouver, BC V6T 1Z4, Canada

Introduction

Grafting, where tissues from one plant genotype are inserted into those of another genotype, so that the two sets of vascular tissues form a unified set (i.e., viable grafted plant), is widely used for breeding (DongKum et al. 2013), variety renewal (Sabbatini and Howell 2013), germplasm conservation (Benelli et al. 2013), as well as determining the genetic stability of plants (Jaganath et al. 2014). It is also employed in plant propagation, including trees (Sanou et al. 2004; Mencuccini et al. 2007), vegetables (Kubota et al. 2008), and flowers (Ginova et al. 2012). Moreover, it is an important method applied in studies addressing shoot–root physiological relationships (Sakamoto and

Nohara 2009; Han et al. 2013), resistance mechanisms (Sugawara et al. 2013), material transport (Lin et al. 2007; Flaishman et al. 2008; Zhang et al. 2012), flowering regulation (Yoo et al. 2013), and long-distance signal transmission mechanisms (Chen et al. 2006; Banerjee et al. 2009).

The nurse seedling grafting is a shoot grafting method characterized by the use of young seedlings, with or without leaves, as the rootstock onto which half-lignified branches (scions) are grafted (Moore 1963). Young shoot tissue is particularly well suited for grafting due to its high cell division activity and the high affinity with which several functional phloem and xylem tissues of the scion-rootstock can connect across the graft surface (Gökbayrak et al. 2007). Nurse grafting can make the grafting body easier to survive, thus suitable for propagation of endangered plants and commercial breeding (Sui 2006; Fuentes et al. 2014). The shoot grafting technique has been applied to a number of plant species, such as camellia (Moore 1963), avocado (Whiley et al. 2007), chestnut (Duman and Serdar 2006), ginkgo, and oak (Park 1968), with camellia as the most extensively studied species.

Successful grafting starts by the healing process between the rootstock and the scion. Healing is capable of initiating such cellular responses by triggering various intracellular signaling events (León et al. 2001; Minabayeva et al. 2015; Sophors et al. 2016). Grafting generates an impulse to elicit healing mechanism that generates biological response (isolation layer formation, callus differentiation, callus proliferation and connection, cambium differentiation and connection, and conducting tissue differentiation and connection) (Estrada-Luna et al. 2002; Fan et al. 2015). Studies conducted on graft-healing mechanism focused on determining the quantities of various biochemical substances in the scion (Pina and Errea 2005; Aloni et al. 2008; Muneer et al. 2016), enzyme activity (Zarrouk et al. 2010), and endogenous hormone content (Aloni et al. 2008; van Hooijdonk et al. 2011; Yin et al. 2012), all of which vary with the healing stage; however, signaling pathways of grafting healing was seldom reached.

MAPK signaling pathways are known to play a central role in cell proliferation, differentiation, apoptosis, and development (Weihs et al. 2014), and belong to the extracellular signal-regulated kinase (ERK) subfamily (Wang et al. 2011). Multiple MAPK pathways exist in one cell, and each pathway is linked to different upstream signals and downstream substrates. These pathways function independently and interlink to form a complex signal transduction network (Wang et al. 2015). Calcium is also an important second messenger in plant signaling networks

(Shi et al. 2014), to response developmental and environmental stimuli representing signal information to distinct biological responses (Ranty et al. 2016; Wang et al. 2016). The calcium signaling occurs by crosstalk of calcium sensitivity, calcium sensors, and downstream target proteins, and interacts with MAPK signaling pathways (Chuderland and Seger 2008; Liu et al. 2014b).

Recently, evidence for MAPK cascade pathways and calcium signal has been found in the same environmental stimuli, such as drought, cold, wounding, and so on (Cheong and Kim 2010; Shi et al. 2014). However, the knowledge of whether and to what extent MAPK cascade pathways and calcium signaling are involved in graft-healing remains unclear. In the present study, we used camellia (*Camellia oleifera*) young shoots as grafting material to study MAPK cascade pathways and calcium signaling underlying the nurse seedling graft-healing processes. In doing so, we focused on changes in anatomy, physiology, biochemistry, and protein expression with the ultimate objective of improving the shoot grafting method for its use in both production and research applications.

Materials and methods

Experimental materials

Camellia oleifera fruits were collected from a single superior clone (Min48) growing at the Minhou Tongkou State Forest Farm, Fujian Province, China ($26^{\circ}09'$, $119^{\circ}14'$) and were placed in a ventilated room until they naturally opened. Large, plump, shiny seeds were selected and stored indoors in clean, dry river sand until use (the following spring (March)). Seeds were germinated in wet sand that was previously treated with a $1000\times$ thiophanate solution. The sand and seeds were placed in alternating single layers (≈ 10 cm thick), and they were watered at 4–5-day intervals. The germinated seeds were used as grafting rootstock only after reaching a height of ≈ 3 cm (Fig. 1a). The germinated shoot tips were cut, and the stems, which were ≈ 1.5 cm long, were used as rootstock (Fig. 1b, c). The seedling roots were trimmed to approximately 6 cm in length. Robust semi-woody branches from the same plants (i.e., homograft) were employed as scions (≈ 2 – 3 cm long) for cleft grafting (Fig. 1d, e). The seedling nursery site was fertilized with farmyard manure at rate of 1000 kg per acre. The seedbed was 1.0 m wide and 0.15 m high with a surface layer of yellow soil that was covered with a plastic film (Fig. 1f). A sun shelter was installed before grafting with a height of 2 m to provide shading rate of 70–80%.

Fig. 1 *Camellia oleifera* nurse seedling grafting steps:
a rootstock cultivation,
b cutting off part of the shoot and root in rootstock, **c** splitting the stem of rootstock,
d prepared scion, **e** grafted plants, and **f** transplanting to seedbed



Experimental design

In total, 10,000 seedlings were homo-grafted, and planted in the seedbed at a spacing of 2–3 and 10–14 cm within and between rows, respectively. The soil was compacted and soaked with water during planting, and the seed case (autotrophic nutrition source) was exposed on the surface before being covered with a transparent plastic film. The temperature inside the greenhouse was maintained at 28–30 °C.

After the grafted plants were transplanted, random samples were collected at 2-day intervals (days 0–26), after which sampling commenced at 3-day intervals (days 29, 32, and 35), followed by 5-day intervals (days 40 and 45), and finally one additional sample after 10 days (day 55), representing a total of 20 samples. Each sampling date included a total of 300 grafted seedlings. The grafted seedling samples were washed under clean running water, and 1–1.5 cm sections of the stems, including the graft junction, were cut and stored in Ziploc® bags. Sampled seedlings were used for: (1) measurement of enzyme activity, hormone levels, and the abundance of various proteins (frozen in liquid nitrogen and stored at –70 °C), (2) measuring soluble sugar content, cellulose, the chlorogenic acid content, and the relative conductivity rate (stored at –20 °C), and (3) anatomy assays (fixed with a formalin/acetic acid/alcohol (FAA) solution less than 48 h after collection).

Measurement methods

Before each sampling event, withered leaves or scions were discarded. The mortality rate of the grafted seedlings was calculated using the following formula:

$$p_i = n_i / \left(N - \sum n_{i-1} - \sum A_{i-1} \right) \times 100,$$

where p_i is the dynamic mortality rate of grafted seedlings; N is the total number of graft recruits ($N = 10,000$); and i is the times of sampling ($i = 1–20$); A_i is the number of recruits in each grafted sampling ($i = 1–20$); and n_i is the times of grafted seedling withered leaves or scions ($i = 1–20$). After each sampling event, 50 randomly selected grafted seedlings were weighed, and the weight gain was denoted as seedling growth.

Soluble sugar and cellulose contents were determined using the anthrone method (Abidi et al. 2010). This is done by 0.5-mL 2% anthrone solution in 5-mL concentrated sulfuric acid to an aqueous solution of grafting union. The absorbance of the green color of the solution is measured using a UV–Vis spectrophotometer SP-756 (Shanghai Spectrum Instruments Company, China) at 620 and 630 nm and it is proportional to the cellulose content and soluble sugar of the sample, respectively. Microcrystalline cellulose and sugar were used as standards for the calibration. All the measurements were repeated three times.

Chlorogenic acid content was measured with a spectrophotometer (Prigent et al. 2003) using ten graft unions. The samples were weighed, ground in liquid nitrogen, transferred to 10-mL centrifuge tube containing 5 mL 80% methanol, placed in refrigerator at 4 °C after shaking extraction for about 4 h, and centrifuged at 3500 r/min at 4 °C for 8 min, after which the supernatant passed through C-18 solid-phase extraction column (column Steps were 80% methanol, 100% methanol, 100% diethyl ether, and 100% methanol cycle) using 80% methanol as a control and absorbance was measured using 756 UV–visible spectrophotometer at 324 nm wavelength. The absorbance measure is proportional to the chlorogenic acid concentration in the sample after using chlorogenic acid as a

standard for calibration. All the measurements were repeated three times.

Electrical conductivity of the collected samples (1.0 g fresh weight) was determined with a Mettler Toledo Electric Conductivity Meter (Delta 326, precision $\pm 0.5\%$), Samples were cut to equal size pieces, immersed in test tubes with 5-mL distilled water, vacuumed for 20 min, set aside for 1 h at room temperature, during which the tubes were shaken several times. Measurements were recorded as S1 data, and then, the tubes were immediately immersed in boiling water at 100 °C for 10 min, followed by cooling until reaching room temperature. The electrical conductivity was re-assayed and recorded S2 data. All the measurements were repeated three times. The relative electrical conductivity rate was calculated by dividing S1 by S2.

Anatomy assay samples were transferred to a 50% acetone solution for 24 days for tissue softening. Sections of 0.5 cm in length were immersed in an improved Kano fixative (70% alcohol/glacial acetic acid, v/v, 3:1); subjected to vacuum for 20 min; fixed for 24 h; washed with water; dyed with 20% ammonium ferrous sulfate for 30 min; rinsed with water; dyed with hematoxylin, eosin, and 2% fuchsin basic for 24 h; washed with water; treated with ammonia for 5 min for contrast; and then washed with water. The materials were then cut into 10-μm slices via the conventional paraffin slice method. An Optec BDS200-FL inverted biological microscope was used to observe the slices, and photographs were taken with a Canon A650 camera.

For enzyme activity determination, a sample (1.0 g fresh weight) which contained about ten graft unions was placed in a precooled mortar, mixed with a small amount of quartz sand and 5 mL of phosphate buffer solution, and ground to a slurry in an ice bath. The extract was centrifuged at 10,000 rpm for 20 min at 4 °C, and the supernatant was transferred to a test tube and stored in a refrigerator. Superoxide dismutase (SOD) activity was determined using the tetrazolium (NBT) photoreduction method with phosphate buffer solution (0.05 mol/L, pH 7.5); catalase (CAT) activity was calculated using the H₂O₂ method with phosphate buffer solution (0.05 mol/L, pH 7.0) (Basha and Rani 2003); peroxidase (POD) activity was measured using the guaiacol method with phosphate buffer solution (0.05 mol/L, pH 7.0) (Zhang et al. 2005); and L-phenylalanine ammonia-lyase (PAL) activity was determined via the production of cinnamate with phosphate buffer solution (0.1 mol/L, pH 8.8) (Cheng and Breen 1991). Polyphenol oxidase (PPO) activity was assayed according to the pyrocatechin method with phosphate buffer solution (0.1 mol/L, pH 6.8) (Ziyan and Pekyardimci 2004). All measurements parameters were performed in triplicate.

To determine hormone levels, a sample (1.0 g fresh weight) was ground to a slurry in a mortar with 2 mL of sample extraction solution (80% methanol, 1 mmol/L butylated hydroxytoluene, BHT), homogenized in an ice bath, and transferred to a 10 mL test tube. The mortar was then washed with an additional 2 mL of the sample extraction solution, which was added to the sample in the test tube, mixed, and leached at 4 °C for 4 h. The extract was subsequently centrifuged at 3500 rpm for 8 min, and the supernatant was collected. The precipitate was mixed with 1 mL of the sample extraction solution and leached at 4 °C for 1 h. After centrifugation at 3500 rpm for 8 min, the supernatant was combined with the previously collected supernatant, after which the total volume was recorded, and the residue was discarded. The supernatant was then purified using a C18 solid-phase extraction column. Hormone levels were measured using an enzyme-linked immunosorbent assay (ELISA) (Bai et al. 2011). Experiments were carried out in triplicate.

The trichloroacetic acid (TCA)/acetone method was employed to extract proteins from the different developmental stages of grafted unions which were collected on 4, 8, 16, 22, 29, and 35 days after grafting, and protein concentrations were determined using the Bradford method (Wei et al. 2009). Proteins were analyzed via two-dimensional electrophoresis (2-DE) (Larsen et al. 2001), and the resultant 2-DE protein maps were analyzed with Image Master TM 2D Platinum software v 7.0. Experiments were carried out in duplicate. Spots of the levels of the differentially expressed proteins were mapped back to and picked from the duplicate 2D gel, and analyzed using a flight tandem mass spectrometer (4700 Proteomics Analyzer; Applied Biosystems, USA). The laser source was an Nd:YAG laser with a wavelength of 355 nm and an acceleration voltage of 20 kV. The data were sampled using the positive ion and automatic data acquisition modes in the analysis. The peptide mass fingerprinting (PMF) scan range was 700–3500 Da, and the five highest intensity peaks were analyzed via tandem mass spectrometry (MS/MS). The spectra were calibrated with external standard calibration digested myoglobin peptides. Database searches were performed to identify differentially expressed proteins using GPS (Applied Biosystems, USA) and MASCOT (Matrix Science, UK) software. The applied search parameters were as follows: database NCBInr; the retrieval species were Viridiplantae (Green Plants); the data retrieval method was combined; the maximum allowable leakage cut locus was 1; the enzyme was trypsin; the quality error range setting was PMF 100 ppm; MS/MS was 0.6 Da; and peaks of trypsin degradation products and pollutants were removed manually during database retrie-

val. The protein function was determined using the freely accessible NCBInr database associated with proteins in a proteomics results ID list.

Data analyses

The differences in physiological and biochemical parameters in grafting unions were analyzed with one-way analysis of variances (ANOVAs), with time as the independent factor. Comparisons among mean parameter were further determined using Duncan HSD post hoc tests. In addition, correlations between all physiological and biochemical parameters were explored using Pearson product-moment correlations. The correlation between different proteins was also explored by the same method. A principal component analysis (PCA) was also performed for mean physiological and biochemical parameters and different proteins using the following steps: (1) input data were standardized, (2) correlation coefficient matrix R was determined, (3) eigen value of the matrix R was determined, (4) principal component loading matrix was determined based on the standard criteria of an eigen value ≥ 1 and a cumulative contribution rate $\geq 80\%$ (Pizzeghello et al. 2011; Reed et al. 2013) to select the relevant principal components, (5) calculate the weight of times, and (6) main parameters of each principal component based on factor loading ≥ 0.20 were selected and ranked from high to low, and ended at variance contribution rate $\geq 70\%$ (the total of selected variable variance contribution/the total of all variable variance contribution $\times 100\%$). All data were analyzed using the statistical software SPSS (version 18.0).

Results

Developmental stages of camellia shoot graft-healing anatomy

The shoot graft-healing anatomy showed five distinct developmental stages that characterized by: (1) the formation of a dark necrotic tissue layer caused by the mechanical damage during surface cutting which acted as an isolation layer at the wound surface (4 days from grafting; Fig. 2a), (2) the parenchyma cells of the rootstock near the wound, cambium, and pericycle had dedifferentiated and recovered the ability to divide resulting in the formation of a callus (Ci) (8 days after grafting; Fig. 2b), (3) the parenchyma cells under the isolation layer at the scion wound had undergone differentiation into a callus (Ci) that was divided and expanded (Fig. 2c; 16 days after grafting), (4) the callus tissue continued proliferation and filled the junction and creating a callus bridge between the rootstock and the scion (22 days from grafting; Fig. 2d).

This progress ensued by the formation of new vascular cambium cells at the edge of the newly formed callus that were differentiated from the parenchyma cells adjacent to vascular cambium of both the scion and the rootstock, crossed the callus between the scion and the rootstock, and fused (29 days from grafting; Fig. 2e), and (5) finally, the cambium or parenchyma cells differentiated into new vessels and sieve tubes, which reconnected the vessels and sieve tubes damaged by grafting, resulting in the formation of vascular bundles and successful completion of the graft-healing process (35 days from grafting; Fig. 2f).

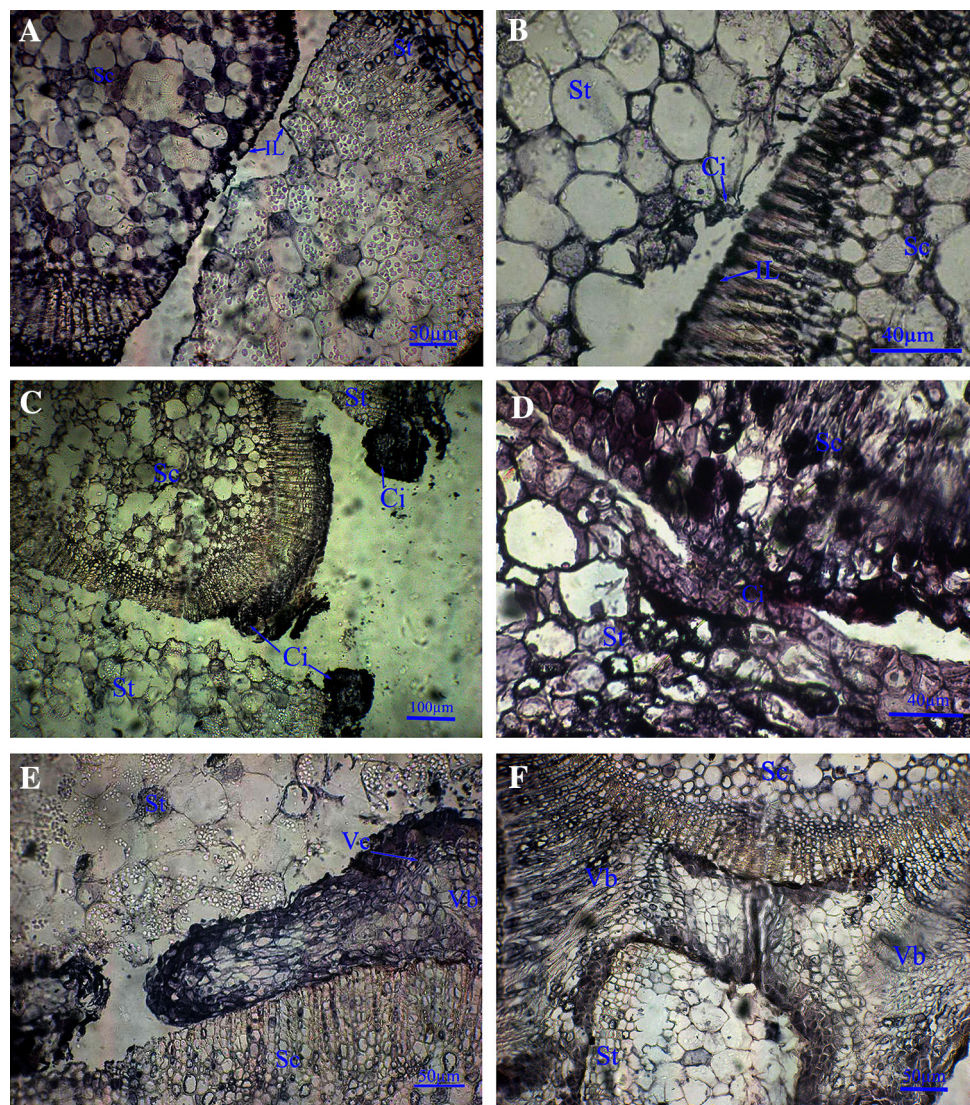
Physiological and biochemical profiles of grafting union development

The analysis of variance identified 15 physiological and biochemical parameters during the development of nurse seedling grafting, all of which were significantly affected by grafting union development ($P < 0.001$). Similarly, the mortality rate also substantially varied and ranged from 0.0 to 5.1% (Table S1). There were peak physiological, biochemical, and mortality rate values at different times after grafting; weight (0 day), ZR (8 day), cellulose, PAL, PPO, and mortality rate (16 day), POD (18 day), CAT (20 day), relative conductivity (22 day), soluble sugar (24 day), SOD (26 day), IAA (29 day), chlorogenic acid content and GA (32 day), and ABA (35 day) (Table S1).

Principal components analysis (PCA) of physiological and biochemical parameters during camellia shoot graft-healing

The first five principal components (PC1–5) of the 15 studied attributes (physiological, biochemical, and mortality rate) during the camellia shoot graft-healing period accounted for 80.92% of the total variation (Table 1). The main parameters of each PC were selected based on their variance contribution [parameters were identified from high to low with cumulative variance contribution reaching $\geq 70\%$ of the total variance (cumulative variance contribution of the selected variable/the total of all variable variance contribution $\times 100\%$)]. PC-1 was mainly influenced by POD, soluble sugars, cellulose content, relative conductivity, chlorogenic acid content, and mortality rate with positive contribution, while seedling weight had negative contribution (Table 1). The cumulative variance contribution of these parameters amounted to 75.35% and accounted for 34.51% of the total variation (Table 1). PC-2 was mainly influenced by GA, ABA, and soluble sugars with positive contribution, and ZR and cellulose content with negative contribution, cumulatively accounting for 70.74% and representing 18.23% of the original data.

Fig. 2 Anatomical analysis of graft union development in *C. oleifera*. **a** Isolation layer (IL) of dark necrotic tissue formed at the wound surface production stage (4 days after grafting), **b** rootstock callus differentiation stage with parenchyma cells near the rootstock (St) wound dedifferentiated to form a callus (Ci) (8 days after grafting), **c** scion callus (Sc) differentiation stage with parenchyma cells at the scion wound differentiated to form a callus (Ci) (16 days after grafting), **d** callus proliferation and connection stage with a callus (Ci) bridge formed between the rootstock and scion (22 days after grafting), **e** vascular cambium (Vc) differentiation and connection stage at the edge of the newly formed callus, 3–4 layers of long, flat vascular cambium cells differentiated from the parenchyma cells (29 days after grafting), and **f** conducting tissue [vascular bundle (Vb)] differentiation and connection stage with the cambium differentiated into a new vessel and sieve tube and reconnected the vessel and sieve tube damaged by grafting, resulting in healing of the grafting union (35 days after grafting)



variation (Table 1). PC-3 accounted for 11.80% of the original variation, and was positively and negatively affected by PPO and chlorogenic acid contents, and CAT and SOD, respectively, with cumulative variance contribution of 79.63% (Table 1). PC-4 accounted for 10.05% of the original variation and was influenced by IAA, SOD, and relative conductivity with positive contribution and PAL and mortality with negative contribution, all with cumulative variance of 89.19% (Table 1). Finally, while PC-5 had an eigen value of <1.0 (0.949), the cumulative variance contribution of PC1–5 accounted for 80.92 of which 6.33% are attributable to PC-5, and thus, it is an important element for the studied 15 attributes detected during the camellia shoot graft-healing period. PC-5 was affected by IAA, morality rate, and cellulose content with positive contribution and ABA and chlorogenic acid content with negative contribution, all representing a cumulative variance contribution of 72.47% (Table 1).

Protein profile and PCA results during the camellia shoot graft-healing process

Using two-dimensional electrophoresis (2DE) and MALDI-TOF-TOF/MS method, a total of 38 differentially expressed proteins were detected from six total proteins at six development stages (4, 8, 16, 22, 29, and 35 days after grafting) during graft-healing process, and identified functions by compared with NCBI database (Table 2).

PCA analysis conducted on the 38 different proteins measured during the six developmental stages of the shoot graft-healing process and based on the standard criteria of an eigen value ≥ 1 and a cumulative contribution rate $\geq 80\%$, identified the first three principal components (PC1–3) as essential and accounted for 85.87% the total variation (Table 3). Main parameters of each PC were selected based on their variance contribution and ranked from high to low with a cut-off factor loading of <0.20, and

Table 1 PCA (PC1–5) of physiological and biochemical parameters during the healing process of camellia shoot grafts

Index	PC1	PC2	PC3	PC4	PC5
Weight	−0.337	0.273	−0.084	0.002	0.171
Cellulose content	0.320	−0.234	0.122	0.144	0.252
Chlorogenic acid content	0.306	0.210	0.390	0.043	−0.228
L-phenylalanine ammonia-lyase (PAL)	0.195	0.171	−0.078	−0.621	0.099
Polyphenol oxidase (PPO)	0.228	0.038	0.493	−0.040	0.121
Peroxidase (POD)	0.392	0.173	−0.102	−0.162	0.133
Superoxide dismutase (SOD)	0.230	0.231	−0.316	0.395	−0.164
Catalase (CAT)	0.210	0.086	−0.549	0.041	0.213
Relative conductivity	0.307	−0.210	−0.193	0.264	0.048
Soluble sugar	0.325	0.307	−0.160	−0.042	−0.209
Mortality rate	0.299	−0.230	0.052	−0.300	0.311
3-Indole acetic acid (IAA)	0.013	0.175	0.210	0.437	0.635
Zeatin (ZR)	0.126	−0.477	−0.049	0.141	−0.170
Gibberellin (GA)	−0.112	0.393	−0.028	−0.011	0.238
Abscisic acid (ABA)	0.175	0.321	0.229	0.185	−0.330
Eigen value	5.177	2.734	1.770	1.508	0.949
VCR (%)	34.51	18.23	11.80	10.05	6.33
Cumulative VCR (%)	34.51	52.74	64.54	74.59	80.92

no-function proteins. PC-1 accounted for 39.59% of the total variation and was positively influenced by calcium-dependent protein kinase (CDPK), glyceraldehyde-3-phosphate dehydrogenase (GAPDH), ribulose 1,5-bisphosphate carboxylase/oxygenase (rubisco), triosephosphate isomerase (TPI), chalcone isomerase (CHI), and fructose-1,6-diphosphate aldolase (ALD), while glutathione transferase (GST), bromodomain protein (BRD), aldehyde reductase (AR), and phenylcoumaran benzylic ether reductase (PCBER) contributed negatively, all with cumulative variance contribution of 63.93% (Table 3). PC-2 accounted for 25.63% of the total variation and was positively affected by mitochondrial ribosomal protein (MRPs), kinesin (centromeric protein)-like protein (CENP), polyubiquitin, heat shock proteins (HSP), membrane-binding steroid protein (MARRS), and negatively by peptidyl-prolyl *cis–trans* isomerase-1 (PPI-1), selenium proteins, germination-like protein, auxin-induced proteins, and oxidative steroid-binding proteins (OSBP), all with cumulative variance contribution of 69.18% (Table 3). PC-3 was associated with 20.65% of the total variation and was positively influenced by cytokinin synthase, copper/zinc superoxide dismutase (Cu-Zn-SOD), translationally controlled tumor protein (TCTP), MARRS, NAD kinase, annexin, peptidyl-prolyl *cis–trans* isomerase-2 (PPI-2), and retrotransposon protein, while PI3K contributed negatively, all with cumulative variance contribution of 59.08% (Table 3).

Discussion

Calcium signal in the vascular bundle development during the camellia shoot graft-healing process

The PC-1 (Table 1) scores were positive between day 14 and 35 and associated with rootstock and scion callus formation, callus connection, and vascular bundle differentiation stages (Table 4; Fig. 2). The PC-1 (Table 3) scores were positive between days 8 and 33 during this time which the union was in the callus formation and vascular bundle differentiation stage (Figs. 2, 3). These indicated that PC-1 (Table 1) and PC-1 (Table 3) were related to the development of the vascular bundle of grafting union. The 7 main indicators of the 17 main indicators in PC-1 (Table 1) and PC-1 (Table 3) (41%) directly were related with calcium signal [POD (Erinle et al. 2016), cellulose content (Lin et al. 2016), chlorogenic acid content (Ngadze et al. 2014), CDPK (Fu et al. 2013), CHI (Li et al. 2004), GST (Dulhunty et al. 2001), and BRD (Zhou et al. 2004)]. Therefore, after grafting, vascular bundle development at the scion may depend on biological responses in which intracellular calcium acts as a second messenger.

In response to grafting, the calcium concentration changed, activating CDPK and the subsequent phosphorylation of the corresponding substrates to cause a signal transduction cascade (Fu et al. 2013). Cell proliferation

Table 2 Relative abundance changes of differentially protein during nurse seedling grafting development (protein function obtained from NCBIInr database)

Name	Protein function	4 days (vol%)	8 days (vol%)	16 days (vol%)	22 days (vol%)	29 days (vol%)	35 days (vol%)
Glutathione transferase (GST)	Cellular processes	0.266	0.153	0.221	0.098	0.036	0.160
Bromodomain transcription factor (BRD)	Chromatin remodeling factors	0.528	0.290	0.241	0.280	0.177	0.494
60s ribosomal protein	Translation	0.147	0.146	0.179	0.069	0.156	0.120
Mitochondrial ribosomal protein (MRPs)	Cell cycle for proliferation	1.076	0.911	1.020	1.460	2.050	1.689
Kinesin (centromeric protein)-like protein (CENP)	Microtubule-based movement	0.158	0.093	0.095	0.000	0.116	0.112
Polyubiquitin	Ubiquitin-dependent protein catabolic process	1.428	1.470	1.160	1.365	2.036	1.885
Heat shock proteins (HSP)	Double-stranded RNA binding	0.114	0.059	0.063	0.080	0.247	0.163
Unknown protein	N/A	0.000	0.374	0.454	0.915	1.833	0.643
Aldehyde reductase (AR)	Carbohydrate metabolic process	0.494	0.054	0.071	0.044	0.056	0.207
Unknown protein	N/A	0.000	0.167	0.271	0.202	0.161	0.292
Phenylcoumaran benzylic ether reductase (PCBER)	NAD(P)-binding domain	2.132	0.596	0.699	1.144	0.806	2.103
Phosphatidylinositol 3-kinase (PI3K)	Signal transducer activity	0.000	0.372	0.554	0.582	0.595	0.905
Homocysteine S-methyltransferase	S-methylmethionine cycle	0.216	0.144	0.158	0.094	0.152	0.273
Cytochrome b-559a subunit	Electron carrier activity	0.000	0.113	0.000	0.000	0.164	0.000
Calcium-dependent protein kinase (CDPK)	Calcium-dependent protein serine/threonine kinase activity	0.000	0.084	0.109	0.000	0.265	0.000
Unknown protein	N/A	0.000	0.181	0.209	0.186	0.432	0.000
Cytokinin synthase	Secondary growth	0.164	0.148	0.127	0.000	0.241	0.000
Copper/zinc superoxide dismutase (Cu-Zn-SOD)	Cellular response to sucrose stimulus	0.510	0.393	0.390	0.589	0.406	0.000
Unknown protein	N/A	0.271	0.045	0.063	0.420	0.726	0.000
Translationally controlled tumor protein (TCTP)	Regulation of mitotic cell cycle	0.319	0.056	0.000	0.057	0.100	0.000
Glyceraldehyde-3-phosphate dehydrogenase (GAPDH)	NADP binding	0.000	0.302	0.326	0.357	0.598	0.000
Ribulose 1,5-bisphosphate carboxylase/oxygenase (Rubisco)	Carbon metabolism	0.000	0.113	0.108	0.000	0.214	0.000
Unknown protein	N/A	0.000	0.093	0.146	0.156	0.381	0.000
Triosephosphate isomerase (TPI)	Carbon metabolism	0.000	0.179	0.173	0.166	0.210	0.000
Chalcone isomerase (CHI)	Biosynthesis of other secondary metabolites	0.000	0.202	0.000	0.000	0.831	0.000
Membrane-binding steroid protein (MARRS)	Negative regulation of cell growth	0.430	0.055	0.067	0.034	0.363	0.000
Unknown protein	N/A	0.000	0.172	0.200	0.223	0.169	0.000
14-3-3 Family protein	Regulation of HS PCII-1-mediated heat shock response	0.000	0.267	0.000	0.000	0.350	0.000
NAD kinase	ATP binding	0.731	0.049	0.045	0.051	0.065	0.000
Annixin	Actin filament binding	0.837	0.396	0.365	0.223	0.271	0.000
Fructose-1,6-diphosphate aldolase (ALD)	Carbon metabolism	0.000	0.169	0.149	0.000	0.318	0.000
Peptidyl-prolyl <i>cis-trans</i> isomerase-1 (PPI-1)	Protein peptidyl-prolyl isomerization	0.000	0.313	0.287	0.256	0.000	0.000
Peptidyl-prolyl <i>cis-trans</i> isomerase-2 (PPI-2)	Protein peptidyl-prolyl isomerization	0.275	0.151	0.218	0.131	0.000	0.000
Selenium proteins	Cell redox homeostasis	0.000	0.286	0.150	0.087	0.000	0.000

Table 2 continued

Name	Protein function	4 days (vol%)	8 days (vol%)	16 days (vol%)	22 days (vol%)	29 days (vol%)	35 days (vol%)
Germination-like protein	Transporter and signal	0.000	0.199	0.276	0.393	0.000	0.000
Auxin-induced protein	Plant hormone signal transduction	0.000	0.148	0.207	0.000	0.000	0.000
Oxysterol-binding protein (OSBP)	Cholesterol binding	0.000	0.052	0.053	0.000	0.000	0.000
Retrotransposon protein	Cell differentiation	0.184	0.121	0.000	0.000	0.000	0.000

was promoted by the inhibition of BRD activity in response to calcium signal stimulation (Zhou et al. 2004; Korner and Tibes 2008; Sterner et al. 1999). It is qualified by the presence of two indicators (CDPK, positive contribution; BRD, negative) in PC-1 (Table 3). Then, intracellular calcium can increase the glycolytic pathway (Vaz et al. 2016; Hoque et al. 2012). Glucose (soluble sugars) can be degraded into dihydroxyacetone phosphate (DHAP) and GAPDH in the presence of ALD. At the same time, DHAP is converted into phosphoglycerate (PGA) in the presence of TPI and GAPDH (Ikemoto et al. 2003). PGA is converted into phosphoenolpyruvate (PEP) with entering into second metabolism (Facchinelli and Weber 2011). Calcium can increase the second metabolism, to produce the chlorogenic acid (Ngadze et al. 2014), such as cinnamic acid and coumaric acid (Clifford et al. 2003). Cinnamic acid was dimerized to lignans (Heinonen et al. 2001), and then reduced by PCBER to other secondary metabolites, such as phytoalexins and heartwood-protective substances (Min et al. 2003). In the presence of POD, lignin and other secondary metabolites participate in cell wall formation, thereby contributing to the development of vascular bundles (Kong et al. 2013). In contrast, coumaric acid is converted to flavonoids in the presence of CHI (Dao et al. 2011). These were qualified by four positive indicators (POD, soluble sugars, cellulose content, and chlorogenic acid content) in PC-1 (Table 1), and by five indicators (GAPDH, TPI, ALD, and CHI; positive; PCBER, negative) in PC-1 (Table 3).

When GST activity reduced, flavonoids increased, and the cell differentiation can be promoted (Kampranis et al. 2000; Laborde 2010), with releasing the material that can be used as carbon source to the new cells, but that also can be transformed to the alcohols by AR. Therefore, reducing the AR can benefit the cell proliferation (Middleton et al. 2000). On the other hand, flavonoids reduce intracellular calcium ion levels, thus activating CDPK (Middleton et al. 2000), thereby contributing to sustained cell proliferation and growth. These were certified by GST and AR that were negative contribution in PC-1 (Table 3).

MAPK signaling pathway in callus proliferation during the camellia shoot graft-healing process

The PC-2 (Table 3) scores were positive between days 8 and 22, a time representing the callus formation stage. The maximum values of PC-2 occurred on days 16 a time associated with rapid callus formation (Figs. 2, 3). The PC-3 (Table 1) scores were positive between day 2 and 4 (coinciding with the isolation layer stage), days 10 and 12 (a rapid callus formation of rootstock stage), and days 20 and 26 (rapid callus formation of scion and rootstock) (Table 4; Fig. 2). The PC-5 (Table 1) score fluctuated dramatically throughout the shoot–rootstock healing development period with high scores corresponding to the five grafting steps (expect vascular bundle differentiation), and with before and after cells growth of callus (Table 4; Fig. 2). Therefore, PC-2 (Table 3), PC-3 (Table 1), and PC-5 (Table 1) were related with callus proliferation during the camellia shoot graft-healing process. The main indicators of them took part in cell proliferation. The 10 main indicators of 18 main indicators in PC-2 (Table 3), PC-3 (Table 1), and PC-5 (Table 1) (56%) directly were related with MAPK signaling pathway [polyubiquitin (Chen et al. 2015), HSP (Svensson et al. 2013), MARRS (Wagatsuma and Sakuma 2014), PPI-1 (Zhimin and Hunter 2014), selenium proteins (Bi et al. 2016), OSBP (Weber-Boyyat et al. 2013), PPO, CAT and IAA (Zheng et al. 2015), and ABA (Wang et al. 2005)]. Therefore, after grafting, callus proliferation may depend on biological responses in MAPK signaling pathway during the camellia shoot graft-healing process.

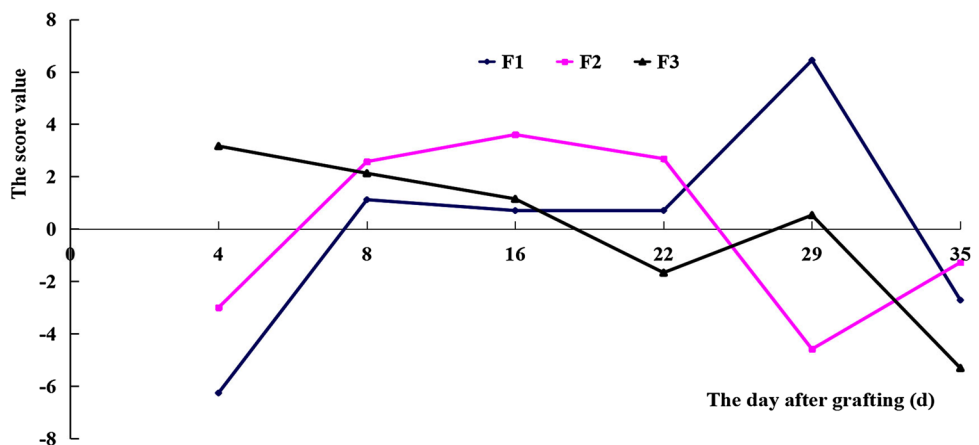
When cells are stimulated by grafting, OSBP interacts with membrane cholesterol, resulting in increased extracellular signal-regulated kinase (ERK) levels which change in cellular calcium concentration (Weber-Boyyat et al. 2013), corresponding signaling cascade by the ubiquitination process, and regulating auxin-induced protein (Chen and Kao 2012; Dharmasiri and Estelle 2004; Schroepfer 2000). By reducing auxin-induced protein, this can increase the levels of free IAA and the polyubiquitin

Table 3 PCA (PC1–3) of the contents of different proteins during the camellia shoot grafts healing process (protein function obtained from NCBIInr database)

Protein	Protein function	PC1	PC2	PC3
Glutathione transferase (GST)	Cellular processes	−0.216	−0.065	0.121
Bromodomain transcription factor (BRD)	Chromatin remodeling factors	−0.240	0.087	−0.070
60s ribosomal protein	Translation	0.031	0.051	0.192
Mitochondrial ribosomal protein (MRPs)	Cell cycle for proliferation	0.127	0.204	−0.198
Kinesin (centromeric protein)-like protein (CENP)	Microtubule-based movement	−0.087	0.203	0.122
Polyubiquitin	Ubiquitin-dependent protein catabolic process	0.091	0.247	−0.155
Heat shock proteins (HSP)	Double-stranded RNA binding	0.100	0.280	−0.099
Unknown protein	N/A	0.220	0.124	−0.098
Aldehyde reductase (AR)	Carbohydrate metabolic process	−0.216	0.158	0.081
Unknown protein	N/A	0.089	−0.151	−0.253
Phenylcoumaran benzylic ether reductase (PCBER)	NAD(P)-binding domain	−0.206	0.152	−0.127
Phosphatidylinositol 3-kinase (PI3K)	Signal transducer activity	0.105	−0.040	−0.313
Homocysteine S-methyltransferase	S-methylmethionine cycle	−0.150	0.150	−0.131
Cytochrome <i>b</i> -559a subunit	Electron carrier activity	0.196	0.118	0.104
Calcium-dependent protein kinase (CDPK)	Calcium-dependent protein serine/threonine kinase activity	0.219	0.109	0.099
Unknown protein	N/A	0.247	0.031	0.079
Cytokinin synthase	Secondary growth	0.099	0.148	0.269
Copper/zinc superoxide dismutase (Cu–Zn-SOD)	Cellular response to sucrose stimulus	0.033	−0.056	0.245
Unknown protein	N/A	0.146	0.178	0.059
Translationally controlled tumor protein (TCTP)	Regulation of mitotic cell cycle	−0.127	0.176	0.212
Glyceraldehyde-3-phosphate dehydrogenase (GAPDH)	NADP binding	0.246	−0.014	0.075
Ribulose 1,5-bisphosphate carboxylase/oxygenase (Rubisco)	Carbon metabolism	0.218	0.064	0.126
Unknown protein	N/A	0.239	0.075	0.051
Triosephosphate isomerase (TPI)	Carbon metabolism	0.229	−0.112	0.101
Chalcone isomerase (CHI)	Biosynthesis of other secondary metabolites	0.204	0.185	0.061
Membrane-binding steroid protein (MARRS)	Negative regulation of cell growth	−0.014	0.248	0.210
Unknown protein	N/A	0.191	−0.184	0.073
14-3-3 Family protein	Regulation of HS PCII-1-mediated heat shock response	0.192	0.107	0.109
NAD kinase	ATP binding	−0.174	0.137	0.200
Annixin	Actin filament binding	−0.115	0.055	0.309
Fructose-1,6-diphosphate aldolase (ALD)	Carbon metabolism	0.219	0.070	0.125
Peptidyl-prolyl <i>cis</i> – <i>trans</i> isomerase-1 (PPI-1)	Protein peptidyl-prolyl isomerization	0.057	−0.301	0.084
Peptidyl-prolyl <i>cis</i> – <i>trans</i> isomerase-2 (PPI-2)	Protein peptidyl-prolyl isomerization	−0.141	−0.117	0.254
Selenium proteins	Cell redox homeostasis	0.051	−0.246	0.129
Germination-like protein	Transporter and signal	0.050	−0.282	0.012
Auxin-induced protein	Plant hormone signal transduction	0.040	−0.226	0.138
Oxysterol-binding protein (OSBP)	Cholesterol binding	0.043	−0.225	0.147
Retrotransposon protein	Cell differentiation	−0.152	0.056	0.241
Eigen value		15.045	9.741	7.845
VCR (%)		39.59	25.63	20.65
Cumulative VCR (%)		39.59	65.22	85.87

Table 4 PCA scores of physiological and biochemical parameters during the healing process in camellia shoot grafts

Time after grafting (days)	PC1	PC2	PC3	PC4	PC5
0	−4.549	1.282	−0.258	0.938	2.062
2	−3.379	−0.832	0.733	−0.963	−0.270
4	−2.978	−0.739	0.544	−0.996	−0.733
6	−1.205	−1.646	−0.410	0.476	0.278
8	0.841	−3.629	−1.166	1.397	−1.440
10	−0.757	−2.623	1.066	0.550	0.360
12	−0.364	−1.357	0.539	−0.315	−0.356
14	1.094	−1.577	−0.027	−1.774	0.860
16	3.707	−1.569	−1.896	−1.554	1.465
18	2.774	0.947	−0.836	−1.939	−0.348
20	1.911	1.547	2.941	−0.492	1.075
22	1.757	−0.163	3.047	0.498	0.288
24	0.999	1.556	0.646	−0.151	−1.174
26	1.919	1.119	0.839	1.185	−1.807
29	1.639	0.423	−1.153	2.870	1.033
32	1.961	2.221	−1.106	0.320	0.014
35	0.637	1.536	−1.250	0.676	−0.019
40	−1.066	0.623	−0.266	0.402	−0.312
45	−2.177	0.940	−0.627	0.541	−0.154
55	−2.765	1.942	−1.360	−1.669	−0.823

Fig. 3 PCA score diagram for different proteins during the healing process of *C. oleifera* shoot grafts

(Dharmasiri and Estelle 2004). And PPI-1 activity was decreased by the ubiquitylation (Zhimin and Hunter 2014). These were confirmed by three main indicators (polyubiquitin, positive contribution; PPI-1 and auxin-induced proteins, negative) in PC-2 (Table 3), and by IAA as main positive indicator in PC-5 (Table 1).

With the deceasing PPI-1 activity, MARRS activity was increasing (Bettoun et al. 2002; Farach-Carson and Nemere 2003; Zhimin and Hunter 2014). In addition, selenium proteins, as MARRS receptor (Schütze et al. 1998), can promote the cell proliferation (Zeng 2009; Zhang et al. 2013), and, on the other side, regulate the reduction of CENP that mediates mitotic progress (Cardoso et al. 2015), with the heat shock proteins (HSP) acting upon

transcription (Kochupillai 2008). Then, MRPs are encoded by nuclear genes, are synthesized in the cytosol, and are then imported into mitochondria for assembly (Zhang et al. 2015). These were qualified by the presence of six main indicators (HSP, MARRS, MRPs, and CENP, positive contribution; PPI-1 and selenium proteins, negative) in PC-2 (Table 3).

Cell proliferation can facilitate a series of biochemical metabolic reactions, along with providing energy and materials for cell growth (Venditti et al. 2013), such as chlorogenic acid contents, PPO, and cellulose content. Germin-like proteins can bind carbohydrates such as cellulose to participate in cell wall modification, and, on the other hand, can prevent cell growth through negative

feedback with H_2O_2 (Dunwell et al. 2008; Caliskan et al. 2004), which can be cleared by SOD and CAT (Liu et al. 2014a). Therefore, reducing SOD and CAT activities result in H_2O_2 increase, which can decrease OSBP activity to reduce cells proliferation and can increase ABA level to activate the MAPK signaling pathway for cells differentiation (Wang et al. 2005). These can be confirmed by two main indicators (germination-like protein and OSBP, negative contribution) in PC-2 (Table 3), by four main indicators (chlorogenic acid content and PPO, positive; SOD and CAT, negative) in PC-3 (Table 1), and by two main indicators (cellulose content, positive; ABA, negative) in PC-5 (Table 1).

MAPK signaling pathway in cell differentiation during the camellia shoot graft-healing process

PC-2 scores (Table 4) were positive after day 22 from grafting, a period coincides with the time of cell differentiation stage for vascular bundle development (Table 4; Fig. 2). The PC-3 scores varied dramatically, with 4–22 days after grafting the score decreased to a minimum on 22 days, a period associated with the largest of naive cell, then the cell went into the secondary growth with score rising up to 29 days in which time most of cells completed the secondary growth to form the vascular bundle, and then, the rest of the score decreased again (Figs. 2, 3). These indicated that PC2 (Table 1) and PC-3 (Table 3) were related to cell differentiation. The 7 main indicators of 15 main indicators in PC2 (Table 1) and PC-3 (Table 3) (47%) directly took part in MAPK signaling pathway [GA (Zheng et al. 2015), ABA (Wang et al. 2005), cytokinin synthase (Mishra et al. 2006), MARRS (Wagatsuma and Sakuma 2014), annexin (Shimizu et al. 2012), PPI-2 (Zhimin and Hunter 2014), and PI3K (Manna et al. 2016)]. Therefore, after grafting, cell differentiation may depend on biological responses in MAPK signaling pathway during the camellia shoot graft-healing process.

Negative feedback with cell proliferation increases ABA level (Wang et al. 2005). As the level of ABA increases rapidly in the scion cells, the MAPK signaling pathway is inhibited (Lehto and Olkkonen 2003) and TCTP is activated (Bommer and Thiele 2004), resulting in the arrest of cell division, through regulation of tubulin binding (Liu 2012). These were verified by ABA as main positive indicator in PC-2 (Table 1), and by TCTP as main positive indicator in PC-3 (Table 3).

Decline of MAPK signaling pathway increased PI3K pathway (Manna et al. 2016) and then leads to increased levels of GA, generating secondary messengers (Ca^{2+}) (Day 2008). Increased PPI activity, which specifically catalyzes the phosphorylation of Ser/Thr residues (Ryo et al. 2003), thereby promoting the formation of annexin

fibers in the cell wall (Grewal and Enrich 2009), results in cell elongation (Lee et al. 2002). These were confirmed by GA and ABA as positive indicator in PC-2 (Table 1), by annexin and PPI-2 as positive indicator in PC-3 (Table 3).

Increased GA levels cause increased intracellular Ca^{2+} contents and endonuclease activation induced to protoplast disintegration, and then, the soluble sugar and hydrogen peroxide (H_2O_2) contents increase (Xie et al. 2014). Soluble sugars participate in cell wall formation. Increased H_2O_2 activates SOD, which prevents cell necrosis and maintains H_2O_2 at moderate levels, so that protoplast disintegration can proceed in a controlled manner (Guaragnella et al. 2011). When the GA content reaches a threshold level, retrotransposon protein is induced, which forms a negative feedback loop for the GA signal transduction pathway by PI3K activity reduced. GA induces cytokinin synthase activity, resulting in cytokinin accumulation in the cells and inhibiting transcription acted as another negative feedback loop. Thereby, maintaining the balance between GA and cytokinins can promote the formation of vascular bundles at the scion graft. These were verified by three main indicators (GA and soluble sugars, positive; ZR, negative) in PC-2 (Table 1), by four main indicators (cytokinin synthase, Cu-Zn-SOD and retrotransposon protein, positive; PI3K, negative) in PC-3 (Table 3).

Conclusion

Camellia oleifera nurse seedling graft-healing illustrates the metabolic activities related with calcium singling and MAPK pathway, providing the raw materials and energy required for cell growth and differentiation involved in cell proliferation and differentiation, which can regulate vascular bundle formation and wound healing. The calcium signal transduction pathways were interlinked with metabolic activity providing the basis for grafted union development, and signal transduction pathways directing the development. At the same time, the calcium signal transduction pathways relied on materials and energy metabolism for energy and intermediates. During material and energy metabolism, there are two key points; namely, (1) BRD initiated the glycolytic pathway that provided ATP and cell components for grafted union and (2) maintaining the balance between CHI and PPO ensuring cell proliferation and subsequent cell differentiation.

Finally, MAPK transduction pathway at the scion consisted of two parts, the first is the transduction of: (1) cell proliferation signal and (2) cells differentiation, with H_2O_2 as the key signal link. In the transduction pathway of the cell proliferation signal, PPI was a key enzyme in the cell proliferation that drove cells from the arrested state into a

division cycle. In the cell differentiation signal, GA was the key point, and its level determined the differentiation state.

Author contribution statement Conceived and designed the experiment: J-LF, HC, and YAK. Performed the experiment: J-LF. Data collection and figures preparation: J-LF and Z-JY. Data analysis: J-LF and C-PC. Wrote the manuscript: J-LF and YAK.

Acknowledgements The authors acknowledge scientific and technical assistance in MALDI-TOF/MS provided by the Proteome Research Center of Fudan University. We thank Minhou Tongkou State Forest Farm of Fujian Province for serving as our experimental base. We thank the Crop Chemistry Control Laboratory of China Agricultural University for supplying the enzyme-linked immunosorbent assay (ELISA) used in this study. We also thank Prof. Jin-xing Lin of Beijing Forestry University and Prof. Bruce C Larson of University of British Columbia for the help and guidance on the paper.

Compliance with ethical standards

Funding This work was supported by Grants received under the Doctoral Fund of the Ministry of Education of China (20123515110010) and the Foundation of Fu'jian Educational Committee (JA12115).

Conflict of interest The authors declare that they have no conflict of interest.

Open Access This article is distributed under the terms of the Creative Commons Attribution 4.0 International License (<http://creativecommons.org/licenses/by/4.0/>), which permits unrestricted use, distribution, and reproduction in any medium, provided you give appropriate credit to the original author(s) and the source, provide a link to the Creative Commons license, and indicate if changes were made.

References

- Abidi N, Hequet E, Cabrales L (2010) Changes in sugar composition and cellulose content during the secondary cell wall biogenesis in cotton fibers. *Cellulose* 17(1):153–160
- Aloni B, Karni L, Deventurero G, Levin Z, Cohen R, Katzir N, Lotan-Pompan M, Edelstein M, Aktas H, Turhan E (2008) Physiological and biochemical changes at the rootstock-scion interface in graft combinations between *Cucurbita* rootstocks and a melon scion. *J Hortic Sci Biotechnol* 83(6):777–783
- Bai TH, Yin R, Li CY, Ma FW, Yue ZY, Shu HR (2011) Comparative analysis of endogenous hormones in leaves and roots of two contrasting *Malus* species in response to hypoxia stress. *J Plant Growth Regul* 30(2):119–127
- Banerjee AK, Lin T, Hannapel DJ (2009) Untranslated regions of a mobile transcript mediate RNA metabolism. *Plant Physiol* 151(4):1831–1843
- Basha PS, Rani AU (2003) Cadmium-induced antioxidant defense mechanism in freshwater teleost *Oreochromis mossambicus* (Tilapia). *Ecotoxicol Environ Safe* 56(2):218–221
- Benelli C, De Carlo A, Engelmann F (2013) Recent advances in the cryopreservation of shoot-derived germplasm of economically important fruit trees of *Actinidia*, *Diospyros*, *Malus*, *Olea*, *Prunus*, *Pyrus* and *Vitis*. *Biotechnol Adv* 31(2):175–185
- Bettoun DJ, Buck DW, Lu J, Khalifa B, Chin WW, Nagpal S (2002) A vitamin D receptor-Ser/Thr phosphatase-p70 S6 kinase complex and modulation of its enzymatic activities by the ligand. *J Biol Chem* 277(28):24847–24850
- Bi CL, Wang H, Wang YJ, Sun J, Dong JS, Meng X, Li JJ (2016) Selenium inhibits *Staphylococcus aureus*-induced inflammation by suppressing the activation of the NF-κB and MAPK signalling pathways in RAW264.7 macrophages. *Eur J Pharmacol* 780:159–165
- Bommer UA, Thiele BJ (2004) The translationally controlled tumour protein (TCTP). *Int J Biochem Cell Biol* 36(3):379–385
- Caliskan M, Turet M, Cuming AC (2004) Formation of wheat (*Triticum aestivum* L.) embryogenic callus involves peroxide-generating germin-like oxalate oxidase. *Planta* 219:132–140
- Cardoso BR, Roberts BR, Bush AI, Hare DJ (2015) Selenium, selenoproteins and neurodegenerative diseases. *Metalomics* 7(8):1213–1228
- Chen YH, Kao CH (2012) Calcium is involved in nitric oxide-and auxin-induced lateral root formation in rice. *Protoplasma* 249(1):187–195
- Chen A, Komives EA, Schroeder JI (2006) An improved grafting technique for mature *Arabidopsis* plants demonstrates long-distance shoot-to-root transport of phytochelatins in *Arabidopsis*. *Plant Physiol* 141(1):108–120
- Chen IT, Hsu PH, Hsu WC, Chen NJ, Tseng PH (2015) Polyubiquitination of transforming growth factor β-activated kinase 1 (TAK1) at lysine 562 residue regulates TLR4-mediated JNK and p38 MAPK activation. *Sci Rep*. doi:[10.1038/srep12300](https://doi.org/10.1038/srep12300)
- Cheng GW, Breen PJ (1991) Activity of phenylalanine ammonia-lyase (PAL) and concentrations of anthocyanins and phenolics in developing strawberry fruit. *J Am Soc Hortic Sci* 116(5):865–869
- Cheong YH, Kim MC (2010) Functions of MAPK cascade pathways in plant defense signaling. *Plant Pathol J* 26(2):101–109
- Chuderland D, Seger R (2008) Calcium regulates ERK signaling by modulating its protein-protein interactions. *Commun Integr Biol* 1(1):4–5
- Clifford MN, Johnston KL, Knight S, Kuhnert N (2003) Hierarchical scheme for LC-MS n identification of chlorogenic acids. *J Agric Food Chem* 51(10):2900–2911
- Dao TT, Linthorst HJ, Verpoorte R (2011) Chalcone synthase and its functions in plant resistance. *Phytochem Rev* 10(3):397–412
- Day PM (2008) Phosphatidylinositol 3-kinase is a positive regulator of gibberellin signaling. Ph.D. Dissertation. The Pennsylvania State University, Pennsylvania
- Dharmasiri N, Estelle M (2004) Auxin signaling and regulated protein degradation. *Trends Plant Sci* 9(6):302–308
- DongKum P, Su K, WooMoon L, HeeJu L, HakSoon C, EunYoung Y, WonByoung C, HoCheol K, YunChan H (2013) Selection of melon genotypes with resistance to *Fusarium* wilt and *Monosporascus* root rot for rootstocks. *Plant Breed Biotechnol* 1(3):277–282
- Dulhunty A, Gage P, Curtis S, Chelvanayagam G, Board P (2001) The glutathione transferase structural family includes a nuclear chloride channel and a ryanodine receptor calcium release channel modulator. *J Biol Chem* 276(5):3319–3323
- Duman E, Serdar U (2006) A research on shortening the nursery period in grafted chestnut. *Hortic Sci (Prague)* 33(1):16–22
- Dunwell JM, Gibbons JG, Mahmood T, Saqlain Naqvi SM (2008) Germin and germin-like proteins: evolution, structure, and function. *Crit Rev Plant Sci* 27(5):342–375
- Erinle KO, Jiang Z, Ma B, Li J, Chen Y, Ur-Rehman K, Shahla A, Zhang Y (2016) Exogenous calcium induces tolerance to atrazine stress in *Pennisetum* seedlings and promotes photosynthetic activity, antioxidant enzymes and psbA gene transcripts. *Ecotoxicol Environ Safe* 132:403–412
- Estrada-Luna AA, Lopez-Peralta C, Cardenas-Soriano E (2002) In vitro micrografting and the histology of graft union formation

- of selected species of prickly pear cactus (*Opuntia* spp.). Sci Hortic 92(3):317–327
- Facchinelli F, Weber AP (2011) The metabolite transporters of the plastid envelope: an update. Front Plant Sci. doi:10.3389/fpls.2011.00050
- Fan J, Yang R, Li X, Zhao W, Zhao F, Wang S (2015) The processes of graft union formation in tomato. Hortic Environ Biotechnol 56(5):569–574
- Farach-Carson M, Nemere I (2003) Membrane receptors for vitamin D steroid hormones: potential newdrug targets. Curr Drug Targets 4(1):67–76
- Flaishman MA, Loginovsky K, Golobowich S, Lev-Yadun S (2008) *Arabidopsis thaliana* as a model system for graft union development in homografts and heterografts. J Plant Growth Regul 27(3):231–239
- Fu L, Yu X, An C (2013) Overexpression of constitutively active *OscPK10* increases *Arabidopsis* resistance against *Pseudomonas syringae* pv. tomato and rice resistance against *Magnaporthe grisea*. Plant Physiol Biochem 73:202–210
- Fuentes I, Stegemann S, Golczyk H, Karcher D, Bock R (2014) Horizontal genome transfer as an asexual path to the formation of new species. Nature 511(7508):232–235
- Ginova A, Tsvetkov I, Kondakova V (2012) *Rosa damascena* Mill.—an overview for evaluation of propagation methods. Bulg J Agric Sci 18(4):1664–1669
- Gökbayrak Z, Söylemezoglu G, Akkurt M, Çelik H (2007) Determination of grafting compatibility of grapevine with electrophoretic methods. Sci Hortic 113(4):343–352
- Grewal T, Enrich C (2009) Annexins-modulators of EGF receptor signalling and trafficking. Cell Signal 21(6):847–858
- Guaragnella N, Antonacci L, Passarella S, Marra E, Giannattasio S (2011) Achievements and perspectives in yeast acetic acid-induced programmed cell death pathways. Biochem Soc Trans 39(5):1538–1543
- Han Y, Wang YH, Jiang H, Wang ML, Korpelainen H, Li CY (2013) Reciprocal grafting separates the roles of the root and shoot in sex-related drought responses in *Populus cathayana* males and females. Plant Cell Environ 36(2):356–364
- Heinonen S, Nurmi T, Liukkonen K, Poutanen K, Wähälä K, Deyama T, Nishibe S, Adlercreutz H (2001) In vitro metabolism of plant lignans: new precursors of mammalian lignans enterolactone and enterodiol. J Agric Food Chem 49(7):3178–3186
- Hoque TS, Uraji M, Ye W, Hossain MA, Nakamura Y, Murata Y (2012) Methylglyoxal-induced stomatal closure accompanied by peroxidase-mediated ROS production in *Arabidopsis*. J Plant Physiol 169(10):979–986
- Ikemoto A, Bole DG, Ueda T (2003) Glycolysis and glutamate accumulation into synaptic vesicles role of glyceraldehyde phosphate dehydrogenase and 3-phosphoglycerate kinase. J Biol Chem 278(8):5929–5940
- Jaganath B, Subramanyam K, Mayavan S, Karthik S, Elayaraja D, Udayakumar R, Manickavasagam M, Ganapathi A (2014) An efficient in planta transformation of *Jatropha curcas* (L.) and multiplication of transformed plants through in vivo grafting. Protoplasma 251(3):591–601
- Kampranis SC, Damianova R, Atallah M, Toby G, Kondi G, Tsichlis PN, Makris AM (2000) A novel plant glutathione S-transferase/peroxidase suppresses Bax lethality in yeast. J Biol Chem 275(38):29207–29216
- Kochupillai N (2008) The physiology of vitamin D: current concepts. Indian J Med Res 127(3):256–262
- Kong LG, Wang FH, Si JS, Feng B, Zhang B, Li SD, Wang Z (2013) Increasing in ROS levels and callose deposition in peduncle vascular bundles of wheat (*Triticum aestivum* L.) grown under nitrogen deficiency. J Plant Interact 8(2):109–116
- Korner M, Tibes U (2008) 5 histone deacetylase inhibitors: a novel class of anti-cancer agents on its way to the market. Prog Med Chem 46:205–280
- Kubota C, McClure MA, Kokalis-B N, Bausher MG, Rosskopf EN (2008) Vegetable grafting: history, use, and current technology status in North America. HortScience 43(6):1664–1669
- Laborde E (2010) Glutathione transferases as mediators of signaling pathways involved in cell proliferation and cell death. Cell Death Differ 17(9):1373–1380
- Larsen MR, Sørensen GL, Fey SJ, Larsen PM, Roepstorff P (2001) Phospho-proteomics: evaluation of the use of enzymatic dephosphorylation and differential mass spectrometric peptide mass mapping for site specific phosphorylation assignment in proteins separated by gel electrophoresis. Proteomics 1(2):223–238
- Lee S, Cheng H, King KE, Wang WF, He YW, Hussain A, Lo J, Harberd NP, Peng JR (2002) Gibberellin regulates *Arabidopsis* seed germination via *RL2*, a GAI/RGA-like gene whose expression is up-regulated following imbibition. Genes Dev 16(5):646–658
- Lehto M, Olkkonen VM (2003) The OSBP-related proteins: a novel protein family involved in vesicle transport, cellular lipid metabolism, and cell signalling. Biochim Biophys Acta Mol Cell Biol Lipids 1631(1):1–11
- León J, Rojo E, Sánchez-Serrano JJ (2001) Wound signalling in plants. J Exp Bot 52(354):1–9
- Li ZH, Sugaya S, Gemma H, Iwahori S (2004) Effect of calcium, nitrogen and phosphorus on anthocyanin synthesis in ‘Fuji’ apple callus. Acta Hortic 653:209–214
- Lin MK, Belanger H, Lee YJ, Varkonyi-Gasic E, Taoka KI, Miura E, Xoconostle-Cázares B, Gendler K, Jorgensen RA, Phinney B (2007) FLOWERING LOCUS T protein may act as the long-distance florigenic signal in the cucurbits. Plant Cell 19(5):1488–1506
- Lin D, Lopez-Sanchez P, Gidley MJ (2016) Interactions of pectins with cellulose during its synthesis in the absence of calcium. Food Hydrocolloids 52:57–68
- Liu Y (2012) Roles of mitogen-activated protein kinase cascades in ABA signaling. Plant Cell Rep 31(1):1–12
- Liu N, Lin Z, Guan L, Gaughan G, Lin G (2014a) Antioxidant enzymes regulate reactive oxygen species during pod elongation in *Pisum sativum* and *Brassica chinensis*. PLoS One 9(2):1–9
- Liu Z, Wang B, He R, Zhao Y, Miao L (2014b) Calcium signaling and the MAPK cascade are required for sperm activation in *Caenorhabditis elegans*. Biochim Biophys Acta Mol Cell Res 1843(2):299–308
- Manna A, De Sarkar S, De S, Bauri AK, Chattopadhyay S, Chatterjee M (2016) Impact of MAPK and PI3K/AKT signaling pathways on Malabaricone-A induced cytotoxicity in U937, a histiocytic lymphoma cell line. Int Immunopharmacol 39:34–40
- Mencuccini M, Martínez-Vilalta J, Hamid H, Korakaki E, Vanderklein D (2007) Evidence for age-and size-mediated controls of tree growth from grafting studies. Tree Physiol 27(3):463–473
- Middleton E, Kandaswami C, Theoharides TC (2000) The effects of plant flavonoids on mammalian cells: implications for inflammation, heart disease, and cancer. Pharmacol Rev 52(4):673–751
- Min T, Kasahara H, Bedgar DL, Youn B, Lawrence PK, Gang DR, Halls SC, Park H, Hilsenbeck JL, Davin LB (2003) Crystal structures of pinosresino-lariciresinol and phenylcoumaran benzylic ether reductases and their relationship to isoflavone reductases. J Biol Chem 278(50):50714–50723
- Minibayeva F, Beckett RP, Kranner I (2015) Roles of apoplastic peroxidases in plant response to wounding. Phytochemistry 112:122–129
- Mishra NS, Tuteja R, Tuteja N (2006) Signaling through MAP kinase networks in plants. Arch Biochem Biophys 452(1):55–68

- Moore JC (1963) Propagation of chestnuts and camellia by nurse seed grafts. North Nut Growers' Assoc Ann Rep 54:88–89
- Muneer S, Ko CH, Wei H, Chen Y, Jeong BR (2016) Physiological and proteomic investigations to study the response of tomato graft unions under temperature stress. PLoS One 11(6):e0157439
- Ngadze E, Coutinho TA, Icishahayo D, Van der Waals JE (2014) Effect of calcium soil amendments on phenolic compounds and soft rot resistance in potato tubers. Crop Prot 62:40–45
- Park KS (1968) Studies on the juvenile tissue grafting of some special use trees II. An experiment on inverted radicle grafting of crop tree species. Rep Korean J Bot 11:8–17
- Pina A, Errea P (2005) A review of new advances in mechanism of graft compatibility–incompatibility. Sci Hortic 106(1):1–11
- Pizzeghello D, Berti A, Nardi S, Morari F (2011) Phosphorus forms and P-sorption properties in three alkaline soils after long-term mineral and manure applications in north-eastern Italy. Agric Ecosyst Environ 141(1):58–66
- Prigent SVE, Gruppen H, Visser AJWG, van Koningsveld GA, de Jong GAH, Voragen AGJ (2003) Effects of non-covalent interactions with 5-O-caffeoylequinic acid (chlorogenic acid) on the heat denaturation and solubility of globular proteins. J Agric Food Chem 51(17):5088–5095
- Ranty B, Aldon D, Cotelle V, Galaud JP, Thuleau P, Mazars C (2016) Calcium sensors as key hubs in plant responses to biotic and abiotic stresses. Front Plant Sci. doi:[10.3389/fpls.2016.00327](https://doi.org/10.3389/fpls.2016.00327)
- Reed JP, Devlin D, Esteves SRR, Dinsdale R, Guwy AJ (2013) Integration of NIRS and PCA techniques for the process monitoring of a sewage sludge anaerobic digester. Bioresour Technol 133:398–404
- Ryo A, Liou YC, Lu KP, Wulf G (2003) Prolyl isomerase Pin1: a catalyst for oncogenesis and a potential therapeutic target in cancer. J Cell Sci 116(5):773–783
- Sabbatini P, Howell GS (2013) Rootstock scion interaction and effects on vine vigor, phenology, and cold hardiness of interspecific hybrid grape cultivars (*Vitis* spp.). Int J Fruit Sci 13(4):466–477
- Sakamoto K, Nohara Y (2009) Soybean (*Glycine max* [L.] Merr.) shoots systemically control arbuscule formation in mycorrhizal symbiosis. Soil Sci Plant Nutr 55(2):252–257
- Sanou H, Kambou S, Teklehaymanot Z, Dembélé M, Yossi H, Sina S, Djingdia L, Bouvet J-M (2004) Vegetative propagation of *Vitellaria paradoxa* by grafting. Agroforest Syst 60(1):93–99
- Schroepfer GJ (2000) Oxysterols: modulators of cholesterol metabolism and other processes. Physiol Rev 80(1):361–554
- Schütze N, Bachthaler M, Lechner A, Köhrle J, Jakob F (1998) Identification by differential display PCR of the selenoprotein thioredoxin reductase as a 1 α ,25(OH)₂-vitamin D₃-responsive gene in human osteoblasts-regulation by selenite. BioFactors 7(4):299–310
- Shi H, Ye T, Zhong B, Liu X, Chan Z (2014) Comparative proteomic and metabolomic analyses reveal mechanisms of improved cold stress tolerance in bermudagrass (*Cynodon dactylon* (L.) Pers.) by exogenous calcium. J Integr Plant Biol 56(11):1064–1079
- Shimizu T, Kasamatsu A, Yamamoto A, Koike K, Ishige S, Takatori H, Sakamoto Y, Ogawara K, Shiiba M, Tanzawa H, Uzawa K (2012) Annexin A10 in human oral cancer: biomarker for tumoral growth via G1/S transition by targeting MAPK signaling pathways. PLoS One 7(9):e45510
- Sophors P, Kim YM, Seo GY, Huh JS, Lim Y, Koh DS, Cho M (2016) A synthetic isoflavone, DCMF, promotes human keratinocyte migration by activating Src/FAK signaling pathway. Biochem Biophys Res Commun 472(2):332–338
- Stern DE, Grant PA, Roberts SM, Duggan LJ, Belotserkovskaya R, Pacella LA, Winston F, Workman JL, Berger SL (1999) Functional organization of the yeast SAGA complex: distinct components involved in structural integrity, nucleosome acetylation, and TATA-binding protein interaction. Mol Cell Biol 19(1):86–98
- Sugawara K, Shiraishi T, Yoshida T, Fujita N, Netsu O, Yamaji Y, Namba S (2013) A replicase of potato virus X acts as the resistance-breaking determinant for JAX1-mediated resistance. MPMI 26(9):1106–1112
- Sui N (2006) Nurse seed grafting and its study status and application prospect in China. J Ningbo Univ (Nat Sci Eng Ed) 19(4):451–456
- Svensson KJ, Christianson HC, Wittrup A, Bourseau-Guilmain E, Lindqvist E, Svensson LM, Mörgelin M, Belting M (2013) Exosome uptake depends on ERK1/2-heat shock protein 27 signaling and lipid raft-mediated endocytosis negatively regulated by caveolin-1. J Biol Chem 288(24):17713–17724
- van Hooijdonk B, Woolley D, Warrington I, Tustin S (2011) Rootstocks modify scion architecture, endogenous hormones, and root growth of newly grafted 'Royal Gala' apple trees. J Am Soc Hortic Sci 136(2):93–102
- Vaz CV, Marques R, Cardoso HJ, Maia CJ, Socorro S (2016) Suppressed glycolytic metabolism in the prostate of transgenic rats overexpressing calcium-binding protein regucalcin underpins reduced cell proliferation. Transgenic Res 25(2):139–148
- Venditti P, Di Stefano L, Di Meo S (2013) Mitochondrial metabolism of reactive oxygen species. Mitochondrion 13(2):71–82
- Wagatsuma A, Sakuma K (2014) Vitamin D signaling in myogenesis: potential for treatment of sarcopenia. Biomed Res Int. doi:[10.1155/2014/121254](https://doi.org/10.1155/2014/121254)
- Wang PY, Weng J, Anderson RGW (2005) OSBP is a cholesterol-regulated scaffolding protein in control of ERK1/2 activation. Science 307(5714):1472–1476
- Wang J, Li X, Liu Y, Zhao X, Chen C, Tian F (2011) MEK/ERK inhibitor U0126 enhanced salt stress-induced programmed cell death in *Thellungiella halophila* suspension-cultured cells. Plant Growth Regul 63(3):207–216
- Wang NN, Zhao LL, Lu R, Li Y, Li XB (2015) Cotton mitogen-activated protein kinase 4 (GhMPK4) confers the transgenic *Arabidopsis* hypersensitivity to salt and osmotic stresses. Plant Cell Tissue Organ Cult 123(3):619–632
- Wang F, Chen ZH, Liu X, Colmer TD, Zhou M, Shabala S (2016) Tissue-specific root ion profiling reveals essential roles for the CAX and ACA calcium transport systems for hypoxia response in *Arabidopsis*. J Exp Bot. doi:[10.1093/jxb/erw034](https://doi.org/10.1093/jxb/erw034)
- Weber-Boyyat M, Zhong W, Yan D, Olkkonen VM (2013) Oxysterol-binding proteins: functions in cell regulation beyond lipid metabolism. Biochem Pharmacol 86(1):89–95
- Wei C, XiangRong Y, WenYu L, ShaoQuan Z (2009) Analysis of differential proteins of floral reversion buds during different period in longan. J Agric Biotechnol 17(4):722–727
- Weihs AM, Fuchs C, Teuschl AH, Hartinger J, Slezak P, Mittermayr R, Redl H, Junger WG, Site HH, Rünzler D (2014) Shock wave treatment enhances cell proliferation and improves wound healing by ATP release-coupled extracellular signal-regulated kinase (ERK) activation. J Biol Chem 289(39):27090–27104
- Whiley A, Giblin F, Pegg K, Whiley D (2007) Preliminary results from avocado rootstock research in Australia. In: Proceedings of the VIth world avocado congress, vol 11, Chile, pp 12–16
- Xie Y, Zhang C, Lai D, Sun Y, Samma MK, Zhang J, Shen W (2014) Hydrogen sulfide delays GA-triggered programmed cell death in wheat aleurone layers by the modulation of glutathione homeostasis and heme oxygenase-1 expression. J Plant Physiol 171(2):53–62
- Yin H, Yan B, Sun J, Jia P, Zhang Z, Yan X, Chai J, Ren Z, Zheng G, Liu H (2012) Graft-union development: a delicate process that involves cell-cell communication between scion and stock for local auxin accumulation. J Exp Bot 17(4):1–14

- Yoo SJ, Hong SM, Jung HS, Ahn JH (2013) The cotyledons produce sufficient FT protein to induce flowering: evidence from cotyledon micrografting in *Arabidopsis*. *Plant Cell Physiol* 54(1):119–128
- Zarrouk O, Testillano PS, Risueño MC, Moreno MÁ, Gogorzeña Y (2010) Changes in cell/tissue organization and peroxidase activity as markers for early detection of graft incompatibility in peach/plum combinations. *J Am Soc Hortic Sci* 135(1):9–17
- Zeng H (2009) Selenium as an essential micronutrient: roles in cell cycle and apoptosis. *Molecules* 14:1263–1278
- Zhang ZQ, Pang XQ, Xuewu D, Ji ZL, Jiang YM (2005) Role of peroxidase in anthocyanin degradation in litchi fruit pericarp. *Food Chem* 90(1):47–52
- Zhang W-N, Gong L, Ma C, Xu H-Y, Hu J-F, Harada T, Li T-Z (2012) Gibberellic acid-insensitive mRNA transport in *Pyrus*. *Plant Mol Biol Rep* 30(3):614–623
- Zhang S, Li F, Younes M, Liu H, Chen C, Yao Q (2013) Reduced selenium-binding protein 1 in breast cancer correlates with poor survival and resistance to the anti-proliferative effects of selenium. *PLoS One* 8(5):e63702
- Zhang X, Gao X, Coots RA, Conn CS, Liu B, Qian S-B (2015) Translational control of the cytosolic stress response by mitochondrial ribosomal protein L18. *Nat Struct Mol Biol* 22(5):404–410
- Zheng Y, Yang Y, Liu C, Chen L, Sheng J, Shen L (2015) Inhibition of *SIMPK1*, *SIMPK2*, and *SIMPK3* disrupts defense signaling pathways and enhances tomato fruit susceptibility to *Botrytis cinerea*. *J Agric Food Chem* 63(22):5509–5517
- Zhimin L, Hunter T (2014) Prolyl isomerase Pin1 in cancer. *Cell Res* 24(9):1033–1049
- Zhou J, Ma J, Zhang BC, Li XL, Shen SR, Zhu SG, Xiong W, Liu HY, Huang H, Zhou M (2004) BRD7, a novel bromodomain gene, inhibits G1-S progression by transcriptionally regulating some important molecules involved in ras/MEK/ERK and Rb/E2F pathways. *J Cell Physiol* 200(1):89–98
- Ziyan E, Pekyardimci S (2004) Purification and characterization of pear (*Pyrus communis*) polyphenol oxidase. *Turk J Chem* 28:547–558